

Actuation Fatigue and Lifetime of NiTiHf High Temperature Shape Memory Alloys

James Mabe, Alex Demblon, Ibrahim Karaman

Materials Science and Engineering
Texas A&M University, College Station, TX 77843 USA
Email: jim.mabe@tamu.edu

Abstract. As part of NASA's University Leadership Initiative (ULI) program a team of researchers led by Texas A&M University are investigating compact and lightweight shape memory alloy (SMA) actuators to drive real time geometry changes in order to minimize the boom signature of supersonic vehicles across all aircraft configurations and atmospheric conditions. The NiTiHf system of high temperature shape memory alloys (HTSMA) was selected as the baseline alloy for the project. In addition to the higher transformation temperatures the nickel rich NiTiHf compositions possess a significantly improved thermomechanical stability compared to NiTi alloys, while maintaining a comparably high work output. This paper describes the testing done to quantify actuation cycling limits and failure modes of these materials. Alloy composition, microstructure, and thermomechanical cycling parameters have all been shown to affect the extended cycling behavior and lifetime performance of HTSMAs. The impact of each of these parameters on actuation fatigue and extended cycling performance are presented. The most effective and practical method to extend both structural lifetime and stabilize the actuation performance of an HTSMA component is shown to be partial thermal cycling. An order of magnitude increase in actuation fatigue lifetime has been successfully achieved by limiting transformation per cycle through partial heating under load. More importantly, actuation work was kept nearly constant by increasing stress while thermally limiting actuation strain. This has been shown to be more effective at increasing the fatigue life than reducing actuation stress level alone, yielding 5 to 10 times the relative improvement in fatigue life.

Keywords: High Temperature Shape Memory Alloys; Shape Memory Alloys, SMA, NiTiHf, Actuation Fatigue; Partial Transformation; Partial Cycling; Minor Loops.

1. INTRODUCTION

To enable the return to flight of civil supersonic aircraft, vehicle designs must move beyond traditional aerodynamic performance metrics to include the shaping of sonic boom signatures to minimize perceived loudness across a wide range of conditions. A vehicle's Mach, angle of attack, and the atmospheric profile between the aircraft and the ground have all been shown to have a significant impact on perceived loudness. To minimize the impact of the adverse conditions on perceived noise small modifications to the geometry of the vehicle's outer mold line (OML) have been shown restore the vehicle to a low boom state [5].

A multidisciplinary team led by Texas A&M University is investigating commercially viable civil supersonic transport aircraft that can modify their shape during flight under a range of conditions to meet noise and efficiency requirements for overland flight. This project is sponsored under NASA's University Leadership Initiative (ULI) program. Shape memory alloy (SMA) based actuators were selected for the adaptive geometry application as they can enable a compact and lightweight distributed system that can provide real-time shape changes to the outer mold line (OML) maintaining optimal low boom and low drag configurations across all environments and flight conditions [6, 7, 9].

NiTiHf high Temperature SMAs (HTSMAs) were selected as the baseline material. HTSMAs prevent inadvertent actuation, as the martensite finish temperature is below any anticipated operational ambient temperatures for aircraft parts, specified as 85°C. It is also important to minimize the Austenite finish temperature to limit the power needed for full actuation. Additionally, a 100,000 cycle lifetime at actuation strains greater than 2% was specified to support practical commercial applications.

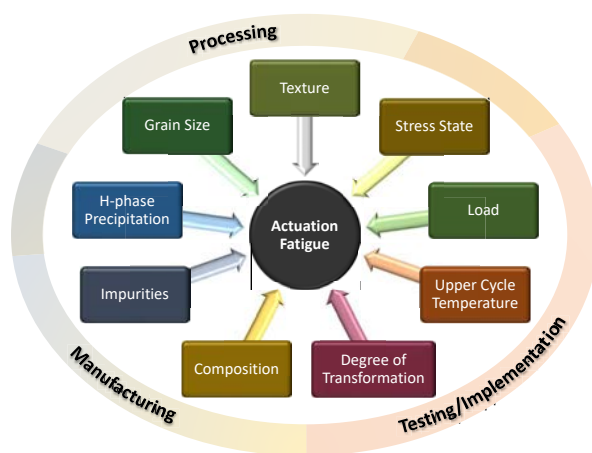


Figure 1: Factors effecting SMA actuation and fatigue performance.

Since its discovery in the 1960s, SMAs have been widely studied and gained significant consideration for actuation applications owing to its robust nature, low weight, high energy density and integration advantages [8]. Ternary NiTi based high temperature SMAs (HTSMAs), such as NiTiZr, NiTiPd, NiTiPT, and NiTiHf, exhibit most of the desired properties of binary NiTi including high work output, corrosion resistance and transformation strain, while also enabling martensitic transformation temperatures up to 500°C. NiTiHf has emerged as a lower cost choice when compared to ternary

HTSMAs with expensive noble metal constituents, including Pt, Pd or Au. The formation of the H-phase precipitates during aging in Ni-rich NiTiHf allows for the setting of transformation temperatures within a wide range and strengthens the matrix against plasticity. However, the sensitivity of shape memory properties to composition in Ni-rich SMA materials remains an inherent problem. A change of just 0.1 at. % of Ni content can alter the transformation temperatures of NiTi materials by as much as 50°C. While maintaining exact composition in the final product is challenging during fabrication of binary Ni-rich NiTi SMAs, it is a bigger challenge for NiTiHf since Hf content needs to be controlled as well. Transformation temperatures, actuation fatigue life cycles and structural stability are affected by the variations between different fabricated batches. Operational parameters, such as upper cycle temperature (UCT) and percentage of full transformation have also been shown to have significant impact on actuation performance. Previous studies on HTSMA have largely been based a single batch

of material at a time. However, when using the same testing parameters for different batches of the same nominal composition that were fabricated with similar processing conditions, a significant variation in actuation fatigue life was observed between batches [1,3,4]. While the issue of reproducibility may not be as critical for laboratory scale experiments, it is regarded as crucial for large scale production.

2. COMPOSITION

The first objective of this study was to investigate batch to batch variations on the actuation and fatigue performance of NiTiHf HTSMAs. To achieve this, four batches of nickel rich material, with a target composition of Ni_{50.3}Ti_{29.7}Hf₂₀ (at. %), were produced via vacuum induction skull melting (VISM). The ingots were homogenized at 1050°C for 72 h in vacuum and then extruded in a single pass at 900°C with an area reduction ratio of 6:1. Compositional analyses of the different batches of as-extruded materials were performed using inductively coupled plasma-atomic emission spectroscopy (ICP-AES) to quantify the matrix composition. C, N, and O concentrations were measured using combustion-infrared absorbance, inert gas fusion-thermal conductivity and inert gas fusion-infrared absorbance, respectively.

Results of the compositional analysis for the different batches of NiTiHf are shown in **Table 1**. All batches differ slightly from the target composition. The measurements for all four batches indicate similar Ni content which is above the target composition and slightly lower than the

Table 1: Batch compositions using ICP-AES

Batch #	Ni (at. %)	Ti (at. %)	Hf (at. %)	Zr (at. %)	C (wt. %)	N (wt. %)	O (wt. %)
1	50.78	29.32	19.2	0.69	0.013	0.002	0.042
2	50.76	29.57	19.43	0.24	0.005	0.002	0.036
3	50.81	29.25	19.67	0.27	0.004	0.000	0.020
4	50.52	29.31	19.8	0.12	0.010	0.001	0.010

target composition for Ti and Hf concentrations. All batches show trace amounts of Zr which is an inevitable contamination in Hf refining. It should be noted that given the tolerances and uncertainties using ICP-AES ($\pm 1\%$ of the absolute level of the element being analyzed) it is difficult to distinguish one batch from the other and from the nominal target compositions.

To further assess and determine the composition of each batch DSC measurements were conducted to determine the stress free transformation temperatures (TT) after solutionization. The DSC results shown in **Fig. 2** indicates large differences between the transformation temperatures of all batches. The effect of Hf on the transformation temperatures of NiTiHf with a constant Ni content is minor compared to the effect of Ni on the transformation temperatures [2]. Therefore, the changes in transformation temperatures (TT) of the NiTiHf due to small changes in Hf content are negligible and the changes are attributed to the changes in Ni content. The DSC results indicate that despite having the same nominal composition, the Ni content is the highest in Batch #4 and lowest in Batch #2 based on the Ni-content dependency of

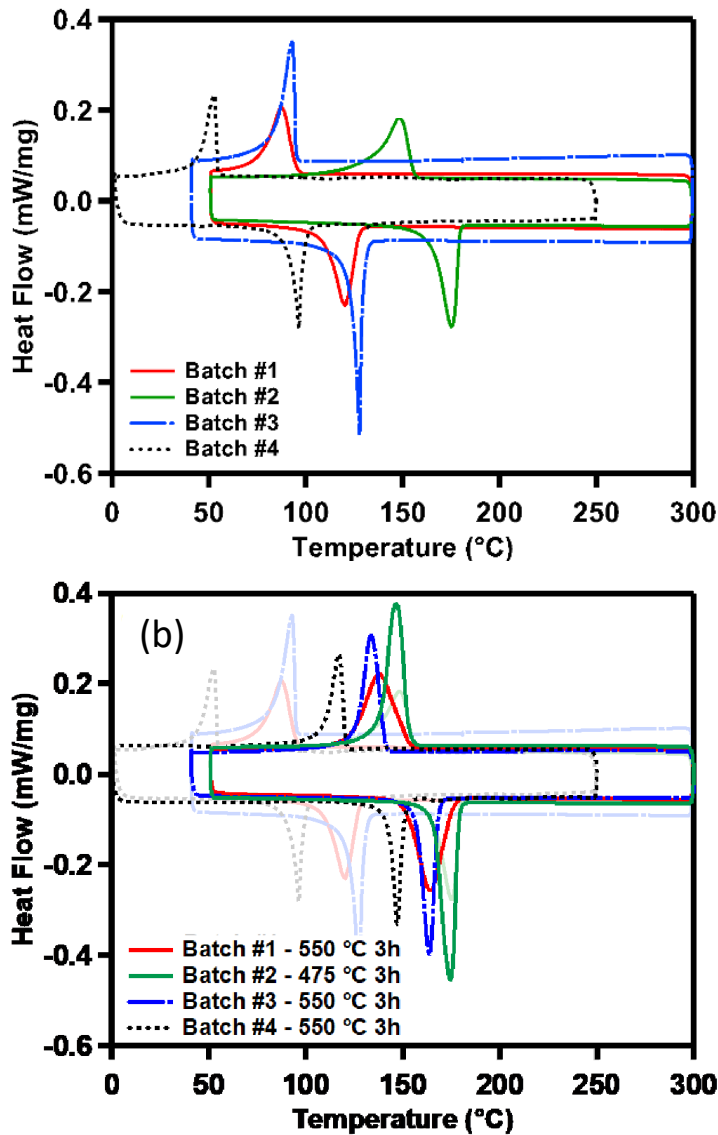


Figure 2: DSC results for 4 batches of NiTiHf

precipitates, microstructures of all batches were investigated using SEM in back-scattered electron (BSE) mode and were found to consist of a NiTiHf matrix with heterogeneously

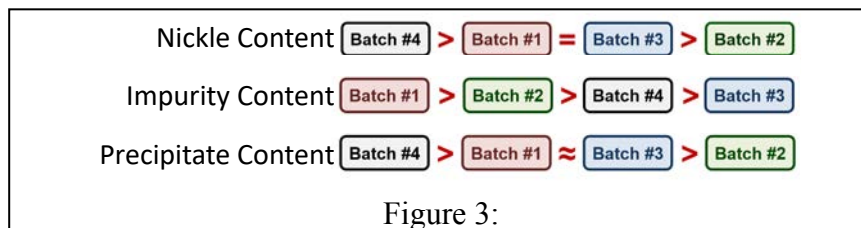


Figure 3:

transformation temperatures. After aging, the transformation temperatures are fairly similar, except for Batch #4 which is about 25°C lower.

Bright-field TEM image analysis was performed to investigate the H-phase precipitate size, morphology and distribution in all of the batches after aging. Precipitates in Batch #1 and #3 are similar in size with an average length of about 15 nm. Precipitates in Batch #4 were slightly smaller, about 13 nm. For Batch #2 (aged at 475°C for 3 hrs to create similar TTs to the other batches) the precipitates were much smaller with an average length and width of about 4.5 nm. Both Batch #1 and #3 had similar, somewhat random distributions of densely populated lenticular precipitates. Batch #4 appears to have even more densely populated precipitates, although they are slightly smaller. This is likely due to the slightly higher Ni content in Batch #4, inferred from the DSC results, which should lead to more precipitate nucleation sites.

In addition to the characterization of H-phase precipitates, microstructures of all batches were investigated using SEM in back-scattered electron (BSE) mode and were found to consist of a NiTiHf matrix with heterogeneously distributed HfO₂, (Ti + Hf)₄Ni₂O_x, and hafnium oxycarbide particles (as identified with energy dispersive X-Ray spectroscopy (EDS)). All batches had

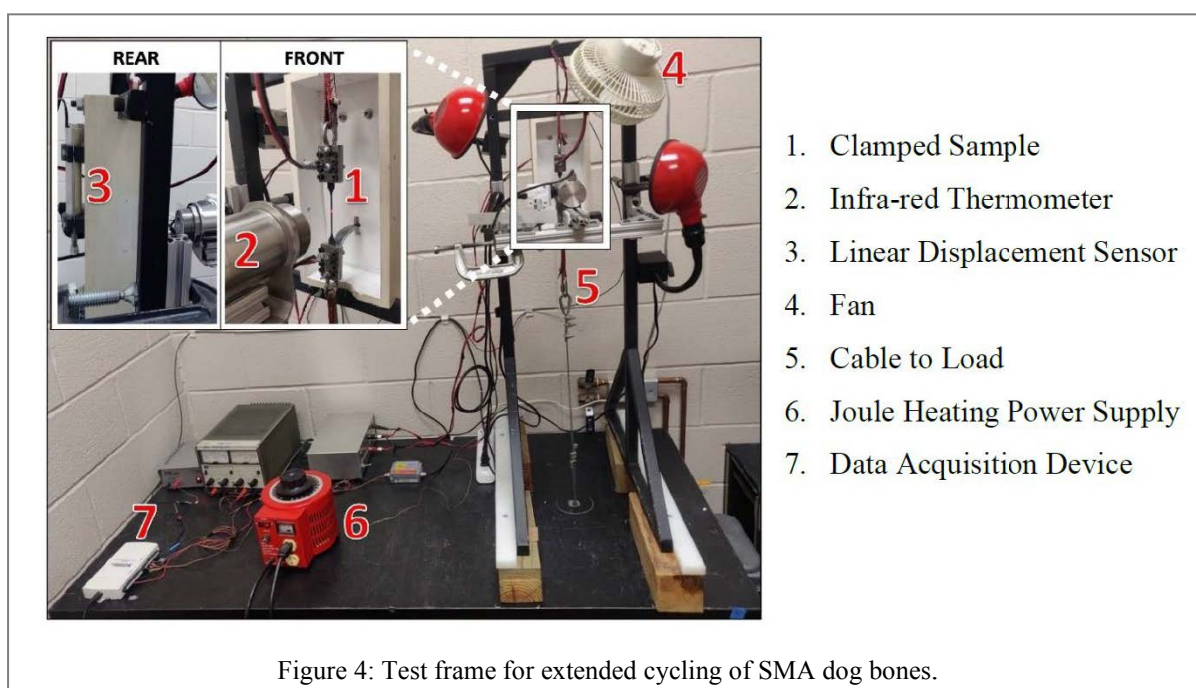
very few and sparsely distributed $(\text{Ti} + \text{Hf})_4\text{Ni}_2\text{O}_x$ particles, particularly in comparison with the amount of hafnium oxide and oxycarbides. The ranking of the batches following chemical, DSC, and microstructure analysis for properties suspected of effecting fatigue are shown in **Fig. 3**.

3. ACTUATION FATIGUE EXPERIMENTS

3.1. Batch to batch variation

Four batches of NiTiHf with the same nominal composition were tested in actuation fatigue experiments to evaluate and compare their durability. Flat dog bone samples with a gauge section 40 mm long, 2.5 mm wide, and 1 mm thick were cut using wire EDM. Actuation fatigue testing was performed using a custom-built apparatus, as shown in **Fig. 4**.

(1) Flat dog bone specimens are clamped in stainless steel friction grips and hung from the



frame. (2) Temperature is measured using an infrared thermometer which is mounted perpendicular to the sample and the samples are painted with a flat black high temperature paint to ensure uniform emissivity. (3) An armature connected to the lower grip extends to the linear displacement sensor which measures the extension of the sample during cycling which is then converted to transformation strain by dividing by the gauge length. (4) A fan is secured to the test frame to convectively cool the sample. (5) A steel cable runs from the bottom grip through the workbench to which weights are hung to achieve the desired load. (6) A variable power supply provides current to joule heat the samples. (7) All devices and sensors are written to and read from the National Instruments NI6211 data acquisition device (DAQ). The

DAQ connects to a computer where the whole experiment is controlled through custom written LabVIEW code.

Fig. 5 illustrates the strain vs. temperature response of different batches during thermo-mechanical cycling under 400 MPa. The evolution of actuation strain, irrecoverable strain, and measured fatigue lives exhibited significant batch to batch variability under the same testing conditions. For all batches, there was a steady increase in total irrecoverable strain until failure. Batches #1 and #4 displayed an increasing actuation strain at each cycle until failure, while Batches #2 and #3 had diminishing values of actuation strain. Batch #2 showed the highest average fatigue life with 10,400 cycles while Batch #4 was the earliest to fail, lasting only 800 cycles. Test were also conducted at 300 MPa with similar results.

The actuation strain vs. cycle for the same data is shown in **Fig. 6**. The decay of actuation strain over cycles suggest the constant UCT is not compensating for the higher driving force required to fully transform as the specimens undergo repeated actuation cycles.

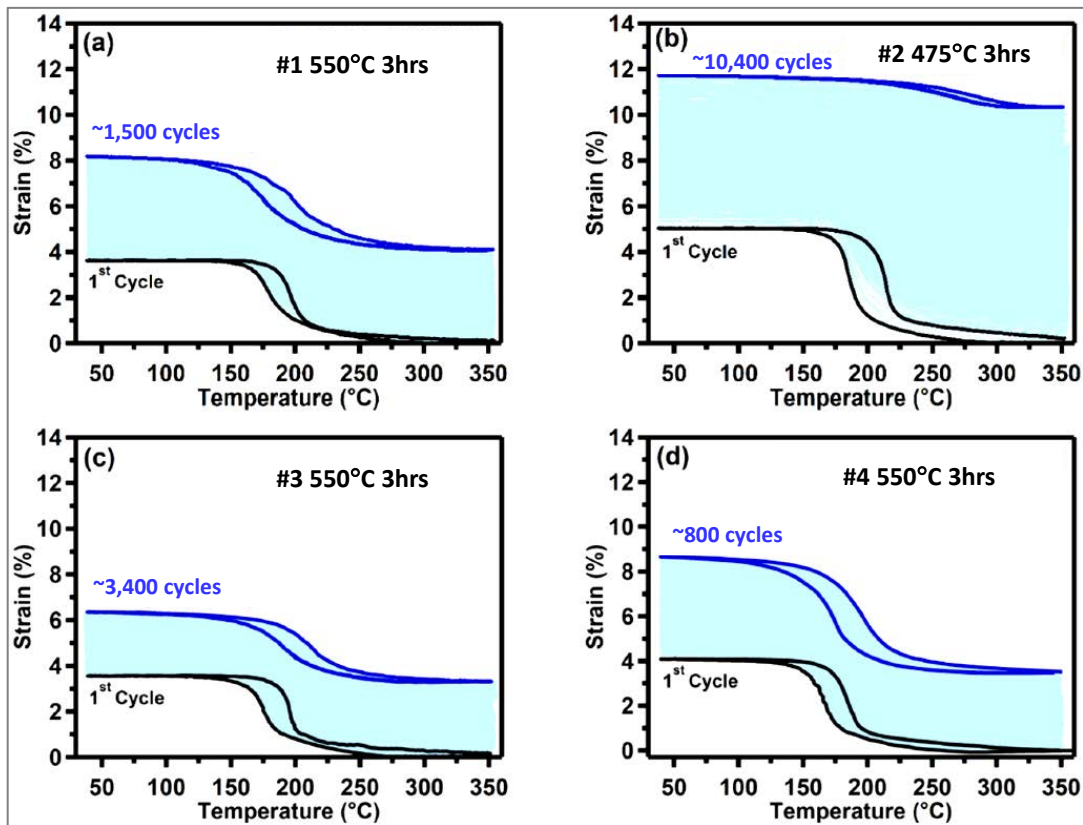


Figure 5: Full transformation strain vs. temperature response of the 4 batches under a 400 MPa load.

3.2. Partial cycling

The second objective of this study was an analysis of the effects of partial cycling compared to full cycling actuation fatigue of Ni50.3Ti29.7Hf. The results indicate an order of magnitude increase in actuation fatigue lifetime can be achieved with partially heated Ni-rich NiTiHf samples. More importantly, keeping actuation work output almost the same by increasing the applied load and controlling actuation strain level by partial cycling was shown to be more effective in increasing the fatigue life than reducing actuation stress level. A 5 to 10 times relative improvement in the fatigue life was observed.

The NiTiHf HTSMA used for this study had a nominal composition of Ni50.3Ti29.7Hf20 (at. %) and was cast via vacuum induction skull melting in a water-cooled Cu hearth. The cast ingots were then homogenized at 1050°C for 72 hrs and furnace cooled before being extruded in a steel can at 900°C to an 8:1 area reduction ratio in one pass. Flat actuation fatigue dog bone samples with a gauge section 40 mm long, 2.5 mm wide, and 1 mm thick were cut using wire EDM and aged at 550°C - 3 hrs in air in the as-extruded condition. Actuation fatigue testing

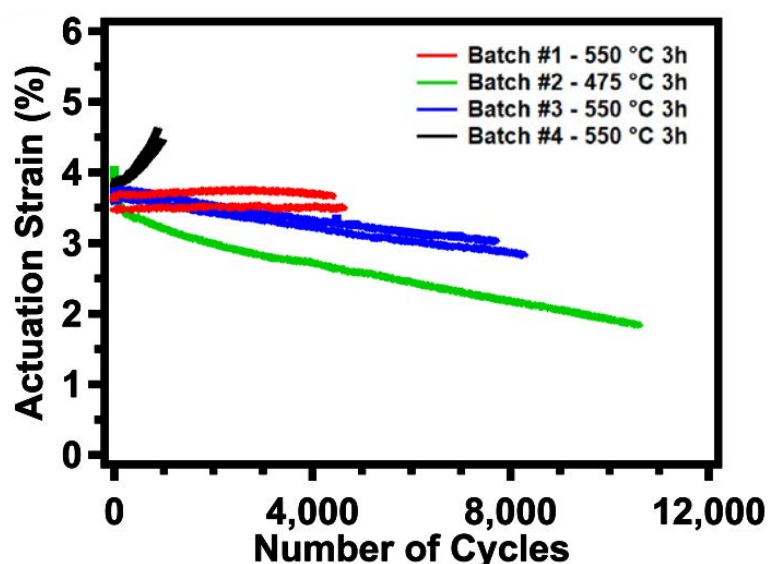


Figure 6 Actuation strain vs. cycles

was performed using the custom-built experimental apparatus, as described above and shown in Figure 4. During actuation fatigue testing samples are loaded to a constant stress and thermally cycled, generating data in the form of strain/temperature hysteresis loops as the material undergoes phase transformation. The idealized strain vs. temperature diagram in Fig. 7 illustrates how the full and partial transformation fatigue tests were performed. One full actuation cycle is defined by cooling from the UCT to the LCT and heating back to the UCT (where UTC is Above A_f and LCT is below M_f), depicted by the dashed blue and red lines, respectively. A partial heating cycle is defined by heating from the LCT to a temperature the generates the targeted strain and cooling back to the LCT, drawn in solid red and blue lines.

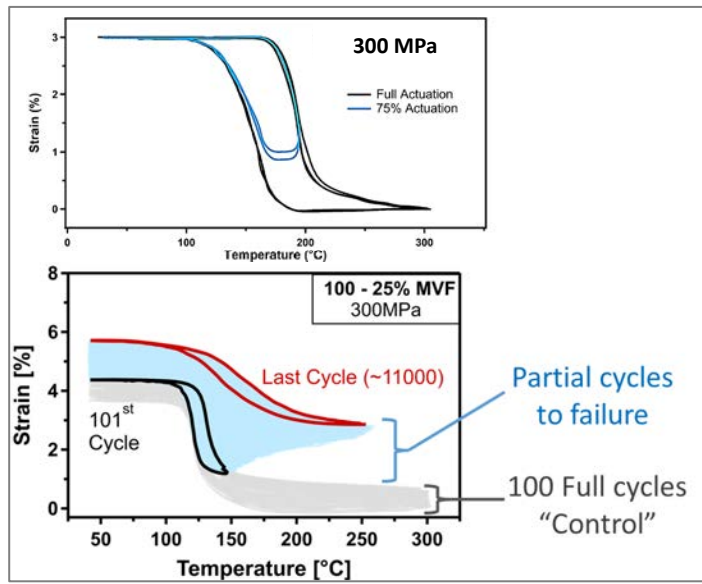


Figure 7: Partial cycling

For extended cycling, all samples were loaded at 300 MPa and tested to four levels of transformation: 100 to 0% martensite volume fraction (MVF), 100 to 10% MVF, 100 to 25% MVF, 100 to 50% MVF and full transformation, 100 to 0% MVF. Initial cycles were performed by cycling the sample between a LCT of 35 °C and UCT of 300 °C for 100 cycles to achieve full transformation, stabilizing actuation and determining the maximum attainable actuation strain.

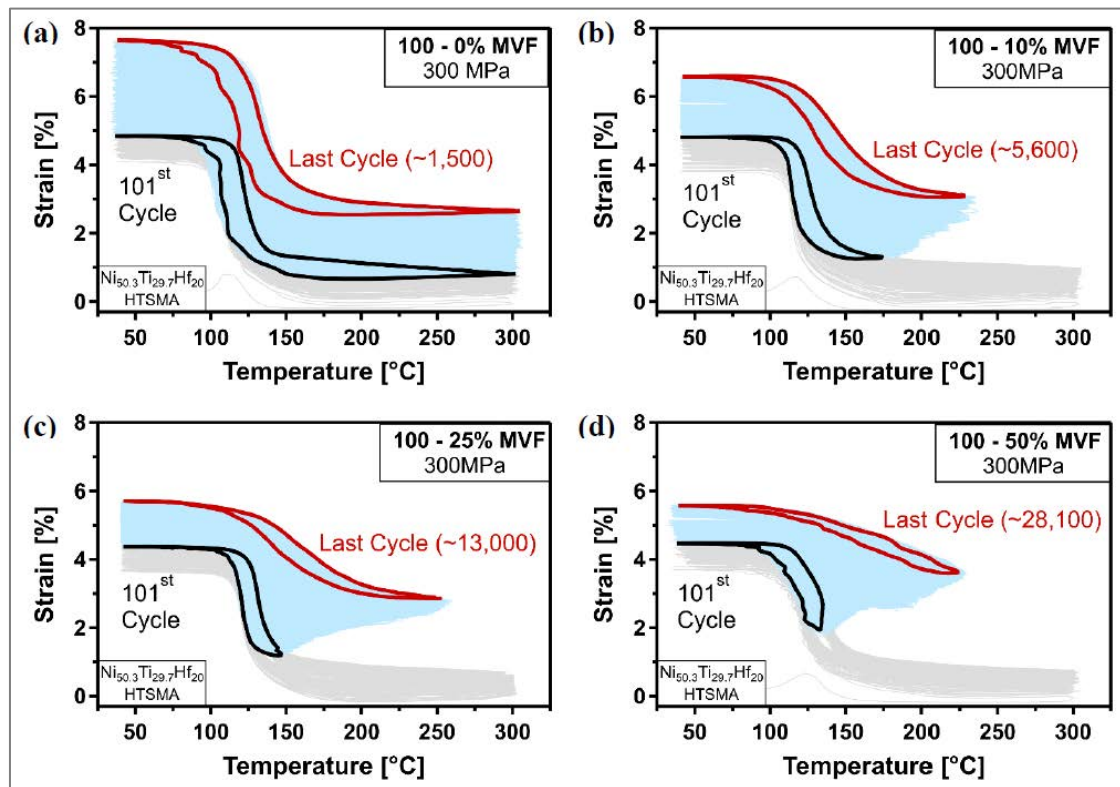


Figure 8: Partial cycling at 300 MPa

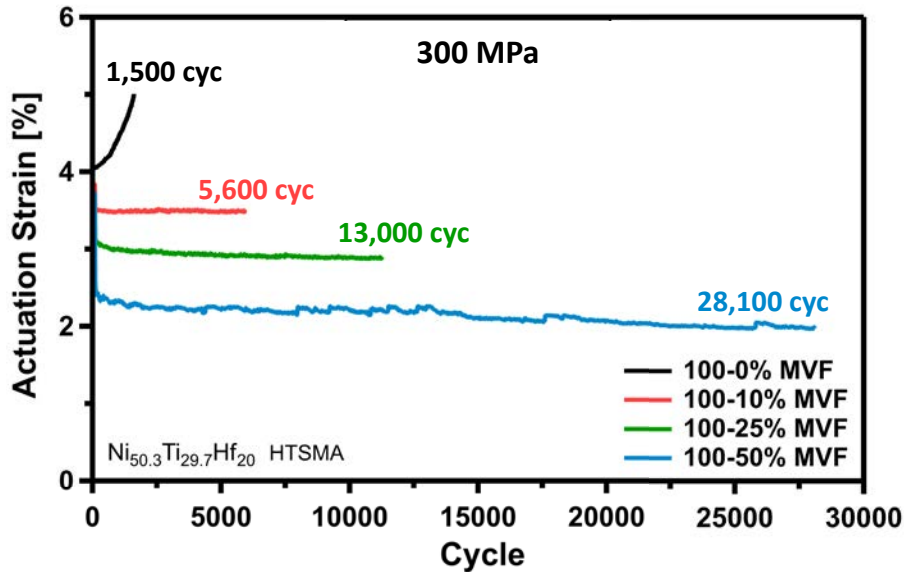


Figure 9: Actuation strain vs. cycles for a range of partial cycle parameters

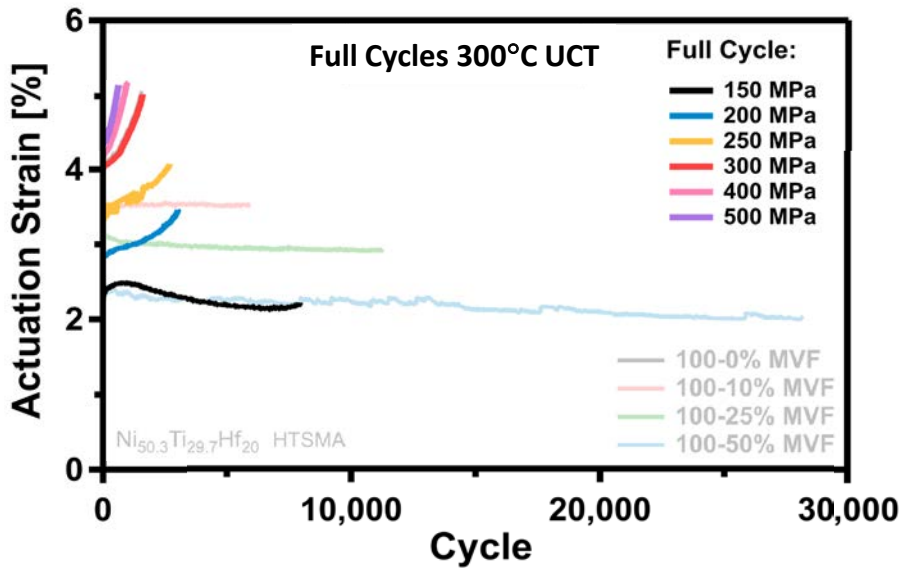


Figure 10: Actuation strain vs. cycles under full transformation for a range of loads.

After 100 cycles the samples were cooled to the LCT and only heated until the desired fraction of maximum actuation strain was reached (i.e., 100%, 90%, 75% or 50% of actuation strain). At least three specimens were cycled under each condition, except for the 100 – 50% MVF case, where only one test was run due to the significant time it took the sample to fail.

As was shown in **Fig. 8** the strain vs. temperature data is crucial in analyzing actuation performance. This data not only illustrates how the austenite, martensite, and actuation strains

evolve over the life of the sample, but shows how transformation temperatures and hysteresis change with an increasing number of cycles.

Representative strain vs. temperature responses for each condition are shown in **Figure 8**. The gray lines show the first 100 control cycles which were run between a fixed LCT and UCT. The stacked light blue lines are the remaining cycles until failure, i.e., from LCT to UCT for 100% transformation and from LCT to partial strain transformation for that test. The 101st cycle (shown in black) is the first partial cycle at each test condition as it is the first cycle after the 100 control cycles. The red line is the last complete cycle before the sample rupture. All four partial cycling ranges are shown in **Fig. 8**. In each case the curves shift up and to the right in small increments with each cycle. This upward shift indicates an increase in plastic deformation causing the sample to elongate over time. The shifting to the right is due to the increase in temperature needed to achieve the same constant actuation strain over time. This suggests that a higher driving force is required to attain the same degree of transformation as the specimens undergo repeated actuation.

The evolution of actuation strain over the life cycles derived from the strain/temperature data is provided in **Fig. 9**. The higher the degree of partial transformation the greater the fatigue life

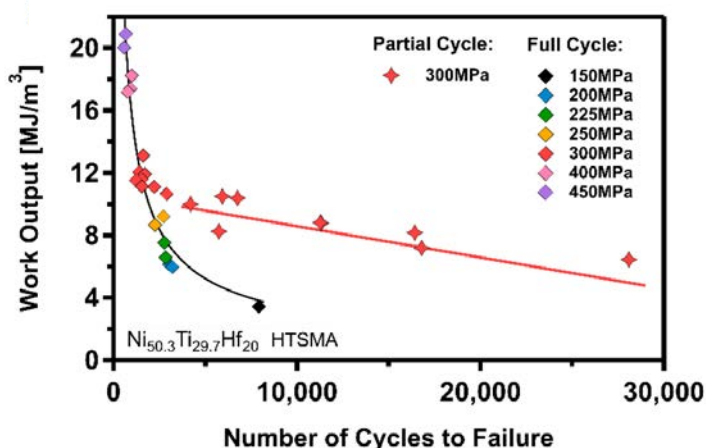


Figure 11: work output vs cycles for full and partial cycling

negative gradient near the beginning of the test and flattening after further cycling (as shown in **Fig. 9** above). With a steep transformation gradient, any small overshoot in temperature (of even a couple of degrees) due to the minor delay between heating and cooling cycles results in a slightly higher actuation strain than was targeted. This effect is less pronounced with the shallower transformation gradient present in later cycles.

3.3. Constant load cycling

To ensure the observed trend of decreasing lifetime with increasing actuation strain was due to partial transformation and not just a factor of actuation strain magnitude (which can be altered by varying loads with a constant UCT) additional experiments were carried out on the same

at the expense of actuation strain. The fully cycled sample was tested under temperature control while the partially cycled tests were conducted under strain control to maintain a constant targeted strain value. In strain control the heating cycle ends when the targeted actuation strain is reached so the actuation strain should remain constant at the targeted value. However, there is a very slight negative slope to the 100 – 25% and 100 – 50% MVF samples due to the A_s to A_f transformation having a steep

material with a fixed UCT of 300°C and applied stresses ranging from 150 MPa to 500 MPa as shown in **Fig. 10** and compares the distinct effects of partial cycling and varying loads on actuation fatigue life cycles. The same data is shown in **Fig. 11** as the average work output vs. life cycles. The work output is calculated as applied load in MPa multiplied by the actuation strain for each cycle and then averaged. This figure clearly shows that small decreases in useful work through partial transformation results in great increases in service life significantly more than when producing similar reduced work output by lessening applied stress. This figure also demonstrates a clear difference in trend when increasing the actuation lifetime by reducing work output through applied stress reduction or partial cycling.

3.4. Additional compositions

To verify the effects of partial cycling applied to other NiTiHf batches and compositions, additional test were run on material with the same hafnium concentration and two lower hafnium concentrations. In **Fig. 12** life

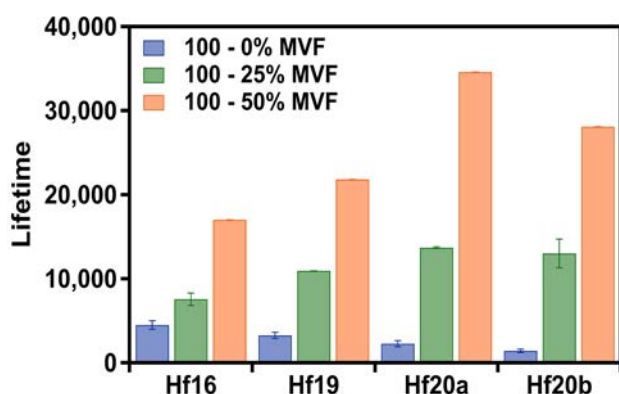


Figure 12: Partial cycling of additional compositions

cycles for each are shown for full transformation cycles and two partial cycle ranges. The data confirms the trends are very similar to the detailed study described above on a single composition and batch.

4. Summary and Conclusions

This study provides insight into the range of behaviors that can be expected within the normal compositional spread that takes place from routine fabrication of multiple batches of NiTiHf SMAs. The

primary objective, to examine the compositional and microstructural sensitivity of the actuation fatigue characteristics of Ni50.3Ti29.7Hf20 (at. %) HTSMA, has been demonstrated through fabrication and testing of four different batches of this nominal composition. The reasons behind the batch to batch variation in actuation fatigue response have been extensively investigated via the diverse set of experiments and different characterization tools to reveal how minor variations can significantly influence the thermomechanical characteristics and performance.

Actuation fatigue experiments were conducted on a nominal Ni50.3Ti29.7Hf20 HTSMA to varying degrees of transformation under a fixed 300 MPa load. Fully cycled samples (100 – 0% MVF) were heated and cooled between a LCT of 45°C (below M_f) and an UCT of 300°C (above A_f). Partially cycled samples were run for 100 “control” cycles under full transformation (LCT to UCT) stabilize actuation and to determine the maximum achievable actuation strain. After the control cycles, the samples were heated from the LCT to a varying PHUCT until the desired fraction of maximum achievable actuation strain was obtained (90%, 75%, and 50%) and run to failure. Analysis of the fatigue data along with post-mortem analysis using SEM, fractography, TEM, and OM led to the following conclusions:

Heating limited partial cycling significantly (more than an order of magnitude) increases the actuation fatigue lifetime in precipitation hardened Ni_{50.3}Ti_{29.7}Hf₂₀. The lower the degree of transformation the longer the lifetime. More importantly, partial thermal cycling and controlling actuation strain results in a much greater increase in fatigue life than lowering the actuation stress level, keeping the actuation work output same.

ACKNOWLEDGMENTS

This work is supported by the NASA University Leadership Initiative (ULI) program under federal award number NNX17AJ96A, titled Adaptive Aerostructures for Revolutionary Civil Supersonic Transportation.

REFERENCES

- [1] A. Demblon, O. Karakoc, J. Sam, D. Zhao, K.C. Atli, J.H. Mabe, I. Karaman, "Compositional and microstructural sensitivity of the actuation fatigue response in NiTiHf high temperature shape memory alloys", *Materials Science and Engineering: A*, Volume 838, 2022, <https://doi.org/10.1016/j.msea.2022.142786>.
- [2] Young, Marcus L., Nathan A. Ley, Skye Segovia, Robert W. Wheeler, Omer Karakoc, Alexander Demblon, and Ibrahim Karaman. "Characterization and Processing of High Temperature Shape Memory Alloys for Aerospace Applications." *AIAA Scitech 2019 Forum* (January 6, 2019).
- [3] Karakoc, O., C. Hayrettin, A. Evirgen, R. Santamarta, D. Canadinc, R.W. Wheeler, S.J. Wang, D.C. Lagoudas, and I. Karaman. "Role of Microstructure on the Actuation Fatigue Performance of Ni-Rich NiTiHf High Temperature Shape Memory Alloys." *Acta Materialia* 175 (August 2019): 107–120.
- [4] J. Mabe, A. Demblon, I. Karaman, "Actuation Fatigue life of NiTiHf High Temperature Shape Memory Alloys", 53431, *ASM International Materials, Applications, and Technologies*, September 2021, St Louis MO.
- [5] Lazzara, David S., Todd Magee, Hao Shen, and James H. Mabe. "Off-Design Sonic Boom Performance for Low-Boom Aircraft." *AIAA Scitech 2019 Forum* (January 6, 2019). doi: <https://doi.org/10.2514/6.2019-0606>
- [6] David S. Lazzara, Todd Magee, Hao Shen, James H. Mabe, Pedro B. Leal and Darren J. Hartl. "A Decoupled Method for Estimating Non-Ideal Sonic Boom Performance of Low-Boom Aircraft Due to Off-Design Flight Conditions and Non-Standard Atmospheres," *AIAA 2021-1271*. *AIAA Scitech 2021 Forum*. January 2021
- [7] Weaver-Rosen, Jonathan M., Pedro BC Leal, Darren J Hartl, and Richard J Malak. "Parametric optimization for morphing structures design: application to morphing wings adapting to changing flight conditions." *Structural and Multidisciplinary Optimization*. July, 2020. doi: <https://doi.org/10.1007/s00158-020-02643-y>
- [8] Calkins, F. T., and Mabe, J. H. (November 16, 2010). "Shape Memory Alloy Based Morphing Aerostructures." *ASME.J. Mech. Des.* November 2010; 132(11): 111012. <https://doi.org/10.1115/1.4001119>
- [9] Jonathan M. Weaver-Rosen, Forrest L. Carpenter, Paul G. Cizmas, Richard J. Malak, Troy A. Abraham, Douglas F. Hunsaker and David S. Lazzara, *Computational Design Methodology of Adaptive Outer Mold Line for Robust Low En-Route Noise of a Supersonic Aircraft*, *AIAA Scitech 2021 Forum*. *AIAA 2021-0877*. January 2021. doi: <https://doi.org/10.2514/6.2021-0877>